Sn (IV) doped lanthanum silicate apatite structure ($La_{9.33}Si_{6-x}Sn_xO_{26}$; x: 0.1; 0.3; 0.5) as an electrolyte

Noviyanti Atiek Rostika[1]*, Eddy Diana Rakhmawaty[1], Hastiawan Iwan[1], Dzulfikar Muhammad[1] and Syarif Dani Gustaman[2]

1. Department of Chemistry, Faculty of Mathematic and Natural Science, Universitas Padjadjaran, Jl. Raya Bandung Sumedang Km.21 Jatinangor 45363, INDONESIA
2. PTNBR – BATAN, Jl. Taman Sari 71 Bandung 40132, INDONESIA
*atiek.noviyanti@unpad.ac.id

Abstract

Conductivities of Sn(IV) doped lanthanum silicates apatite as an electrolyte for intermediate temperature solid oxide fuel cells (ITSOFCs) have been examined. Dense ceramic pellet of $La_{9.33}Si_{6-x}Sn_xO_{26}$ (x: 0.1; 0.3; 0.5) have been prepared by sintering at 1773K for 3 hours. The sample $La_{9.33}Si_{5.7}Sn_{0.3}O_{26}$ shows higher conductivities than comparable $La_{9.33}Si_{5.9}Sn_{0.1}O_{26}$ and $La_{9.33}Si_{5.5}Sn_{0.5}O_{26}$ samples indicating the importance of dopant concentration. Low activation energy of all samples (E_a < 1.1 eV) indicate that the Sn(IV) doped electrolytes are good conductors that can be used for ITSOFCs.

Keywords: Doped lanthanum silicates apatite, ITSOFCs, electrolyte.

Introduction

Lanthanum silicates with an apatite structure are considered as potential candidates for SOFCs operated at intermediate temperature, owing to its high ionic conductivity of 2.95 × 10^{-4} S cm^{-1} at 500°C and low activation energy of about 0.8 eV[1]. The open structure of lanthanum silicate apatite suggests that this material should be appropriate for the electrolyte applications for intermediate temperature SOFCs[2, 3].

The computer modeling studies have indicated the importance of the silicate substructure in aiding the motion of the oxide ions down the channels in the apatite-type oxide ion conductors[4]. The structure of lanthanum silicate apatite is highly tolerance to cation and anion doping. In *P63/m*, $La_{9.33}Si_{6-x}Sn_xO_{26}$ has O1, O2, O3, O4 atoms and the interstitial oxygen O5, located at site [12i; (x, y, z)] near the hexagonal channel proposed from atomistic simulation[5, 6]

Numerous cationic doping were preparation at the Si site, this strategy is helpful to increase the conductivity of apatite lanthanum silicates[7,8]. Substitution of cations with a relatively low valence, Mg^{2+} [8, 9], trivalent such as Al^{3+}, Ga^{3+} has a beneficial effect on conductivity[10]. Doping of cations with a same valence such as Sn^{4+} relative few studies was reported.

Lanthanum silicate apatite doped with tetravalent Sn^{4+} cations at the Si^{4+} site ($La_{10}Si_{5.5}Sn_{0.5}O_{26.75}$) exhibits a similar total conductivity to undoped $La_{10}Si_6O_{27}$[7]. Few studies were carried out on the influence of doping Sn^{4+} with different concentration. In this work, $La_{9.33}Si_{6-x}Sn_xO_{26}$ (x: 0.1; 0.3; 0.5) lanthanum silicate apatites have been prepared by hydrothermal reaction as a first step. Then, the structural characterization of prepared materials has been performed with XRD and refinement techniques using Rietica software. Finally, conductivity properties of the lanthanum silicate apatite have been investigated by complex impedance spectroscopy.

Material and Methods

Synthesis of Sn(IV) doped lanthanum silicates apatite: To prepare the series Sn(IV) doped lanthanum silicates apatite ($La_{9.33}Si_{6-x}Sn_xO_{26}$; x: 0.1; 0.3; 0.5) were prepared from La_2O_3 99.999% (Aldrich), Na_2SiO_3, 97% (Sigma), and SnO_2 99.999% (Sigma-Aldrich). The reactants in the correct stoichiometric ratio were intimately mixed and hydrothermally synthesized at 503 K for 72 h. Phase purity was then examined using powder X-Ray diffraction (Rigaku SmartLab) using Cu-K_α radiation. Ionic conductivity was measured using LCR (GW Instek 61056) at 873 – 973 K and a frequency range of 20 Hz – 5 MHz on the pellet sample that was obtained by applying 6000 kg cm^{-2} pressure followed by sintering at 1773 K for 3 hours.

Results and Discussion

Fig. 1 shows the XRD patterns of apatite-type $La_{9.33}Si_6O_{26}$ ceramics and Sn(IV)-doped series, $La_{9.33}Si_{6-x}Sn_xO_{26}$ (x: 0.1; 0.3; 0.5) ceramics. The main diffraction peaks of various ceramics are in agreement with the standard XRD diffraction of $La_{9.33}Si_6O_{26}$ (ICSD No. 158963)[1].

The lattice parameters of $La_{9.33}Si_{5.9}Sn_{0.1}O_{26}$, $La_{9.33}Si_{5.7}Sn_{0.3}O_{26}$ and $La_{9.33}Si_{5.5}Sn_{0.5}O_{26}$ ceramics are listed in table 1. All the ceramics consist only of a hexagonal apatite structure with a space group *P63/m*, however, all ceramics are composed of a hexagonal apatite structure and a small amount of second phase La_2SiO_5, which is usually characterized by the presence of typical peaks at 2θ values of about 15.48° and 47.26°. Previous studies[1,11] also reported on the difficulty to eliminate La_2SiO_5 phase in lanthanum silicates under most of synthesis and sintering conditions[1]. It is very difficult to find a correlation between Sn content, and the lattice parameter changes. Phase of $La_{9.33}Si_{5.9}Sn_{0.1}O_{26}$ has highest lattice parameter.

The reported cell parameter data are similar with each other, no significant shift is observed in all diffraction pattern of

Sn(IV) doped apatite, as expected size of dopant and host cation. SEM micrograph of $La_{9.33}Si_6O_{26}$ ceramics and Sn(IV)-doped series of ($La_{9.33}Si_{6-x}Sn_xO_{26}$ (x : 0.1 ; 0.3 ; 0.5) ceramics (Fig. 2) show grain and grain boundary region as a function of Sn^{4+}contents.

The homogeneity, porosity and the average grain size decreased when composition of Sn^{4+} is 0.1 and 0.3 but grain size increased at Sn^{4+} 0.5. It is due to effect of the Sn^{4+} content to homogeneity and porosity.

In general, the electrical conductivities of polycrystalline materials are greatly influenced by their microstructures i.e. the properties of grain and grain boundary. AC impedance spectroscopy is widely employed to obtain information related to the electrical behavior of both the bulk (grain interiors) and the grain boundaries. A typical impedance plot for $La_{9.33}Si_6O_{26}$, $La_{9.33}Si_{5.9}Sn_{0.1}O_{26}$, $La_{9.33}Si_{5.7}Sn_{0.3}O_{26}$, and $La_{9.33}Si_{5.5}Sn_{0.5}O_{26}$ is shown in fig. 3.

There is no difference in the curves seen in all four impedance spectra, all dominated by the bulk phase response curve, the bulk resistance globally increases with porosity[12]. Base on the observations of SEM micrographs (Fig. 2), it is very difficult to find a correlation between Sn content, morphology and the resistance of the bulk phases.

Table 2 listed conductivity of $La_{9.33}Si_{5.9}Sn_{0.1}O_{26}$, $La_{9.33}Si_{5.7}Sn_{0.3}O_{26}$ and $La_{9.33}Si_{5.5}Sn_{0.5}O_{26}$ at 873-973 K. Compared with non-doped apatite, all Sn(IV) doped apatites have lower conductivity at all measuring temperatures according to a previous study[7]. Meanwhile, the order of conductivity of Sn(IV) doped apatites from large to small is as follows: $La_{9.33}Si_{5.7}Sn_{0.3}O_{26}$ > $La_{9.33}Si_{5.9}Sn_{0.1}O_{26}$, > and $La_{9.33}$ $Si_{5.5}Sn_{0.5}O_{26}$. It is hard to determine correlation between the change in conductivity to the change of lattice parameters, as well as the ceramic density. Computer simulations technic are required to predict the effect of changes in lattice and morphological parameters on the conductivity of Sn(IV) doped apatite.

Fig. 4 presents the Arrhenius plots of total conductivity of $La_{9.33}Si_{6-x}Sn_xO_{26}$ (x = 0.1; 0.3; 0.5) ceramics. The straight lines are well fitted to the Arrhenius equation which demonstrates that the diffusion process of oxide ions is thermally activated in the range of 873–973 K, which also indicates that the ionic diffusion process is thermally activated.

The activation energy represents the minimum energy required for the oxide-ion diffusion process to happen. The values of activation energy E and pre-exponential factor σ_0 can be determined from the slope and the intercept of the linear. It is in the logarithmic form of the Arrhenius equation for each composition respectively. Activation energy of total conductivity of $La_{9.33}Si_{6-x}Sn_xO_{26}$ (x = 0.1; 0.3; 0.5) ceramics is shown in Table 3.

All values of the activation energy were smaller than 1.1 eV. Low activation energy (<1.1 eV) indicates that $La_{9.33}Si_{6-x}Sn_xO_{26}$ (x = 0.1; 0.3; 0.5) conductivity at 873-973 K is generated from the interstitial oxygen ion migration[13]. These results indicate that both the composite material are good ionic conductors as electrolyte of solid oxide fuel cell.

As seen in table 3 and fig. 4, the activation energies of $La_{9.33}Si_{6-x}Sn_xO_{26}$ (x = 0.1; 0.3; 0.5) are lower than those of $La_{9.33}Si_6O_{26}$. On the other hand, Sn dopant decreases the activation energies, although it will not increase their conductivity.

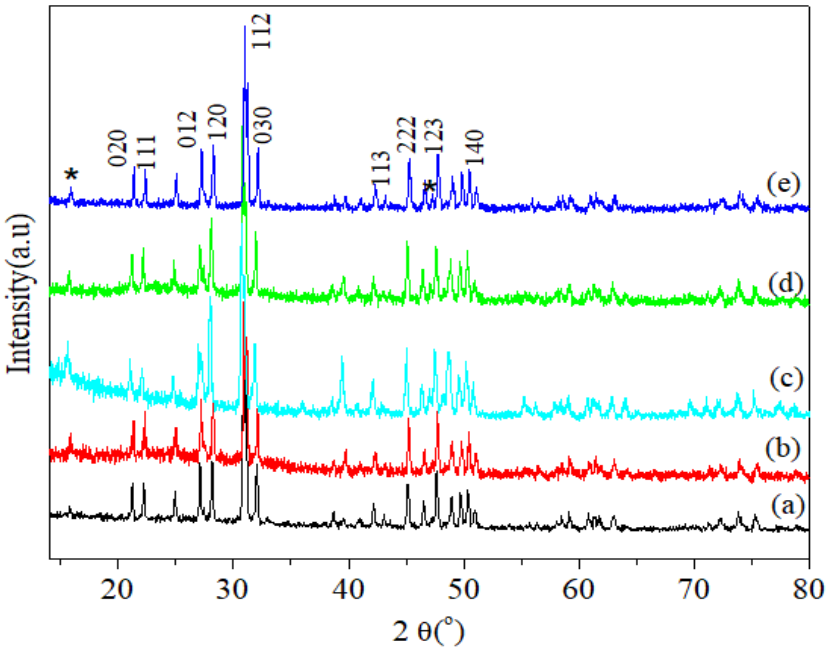

Fig. 1: Diffraction pattern of (a) $La_{9.33}Si_6O_{26}$ (ICSD No. 158963) (b) $La_{9.33}Si_6O_{26}$ (c) $La_{9.33}Si_{5.9}Sn_{0.1}O_{26}$ (d) $La_{9.33}Si_{5.7}Sn_{0.3}O_{26}$ (e) $La_{9.33}Si_{5.5}Sn_{0.5}O_{26}$ and (*) La_2SiO_5.

Table 1
Lattice parameter of $La_{9.33}Si_{6-x}Sn_xO_{26}$ with space group *P 63/m*.

Ceramic	*a*=*b* (Å)	*c* (Å)	Cell Volume (Å)
$La_{9.33}Si_6O_{26}$	9.7187(2)	7.1873(3)	587.9100(1)
$La_{9.33}Si_{5.9}Sn_{0.1}O_{26}$	9.7878(1)	7.2164(1)	598.6843(1)
$La_{9.33}Si_{5.7}Sn_{0.3}O_{26}$	9.7154(1)	7.1767(1)	586.6400(1)
$La_{9.33}Si_{5.5}Sn_{0.5}O_{26}$	9.7188(1)	7.1834(1)	587.6000(1)

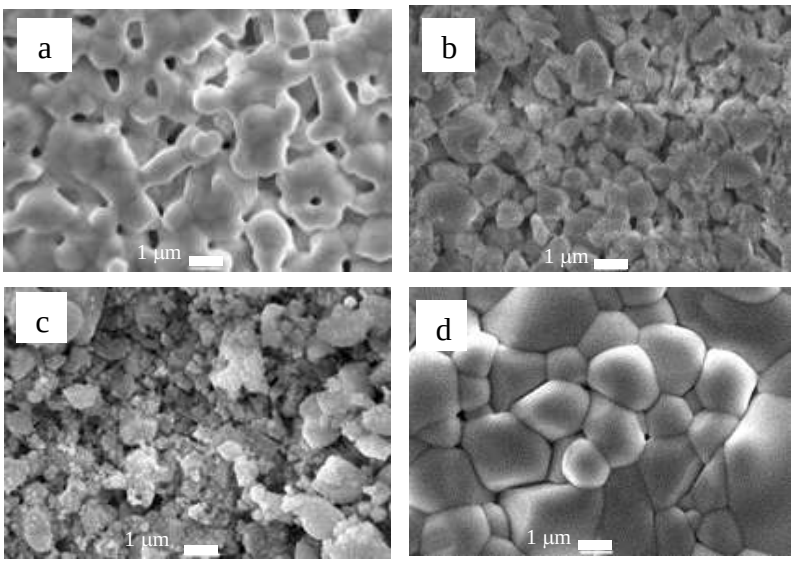

Fig. 2: **SEM micrographs of a) $La_{9.33}Si_6O_{26}$ b) $La_{9.33}Si_{5,9}Sn_{0.1}O_{26}$ c) $La_{9.33}Si_{5.7}Sn_{0.3}O_{26}$ and d) $La_{9.33}Si_{5.5}Sn_{0.5}O_{26}$ after sintered at 1603 K for 3 h.**

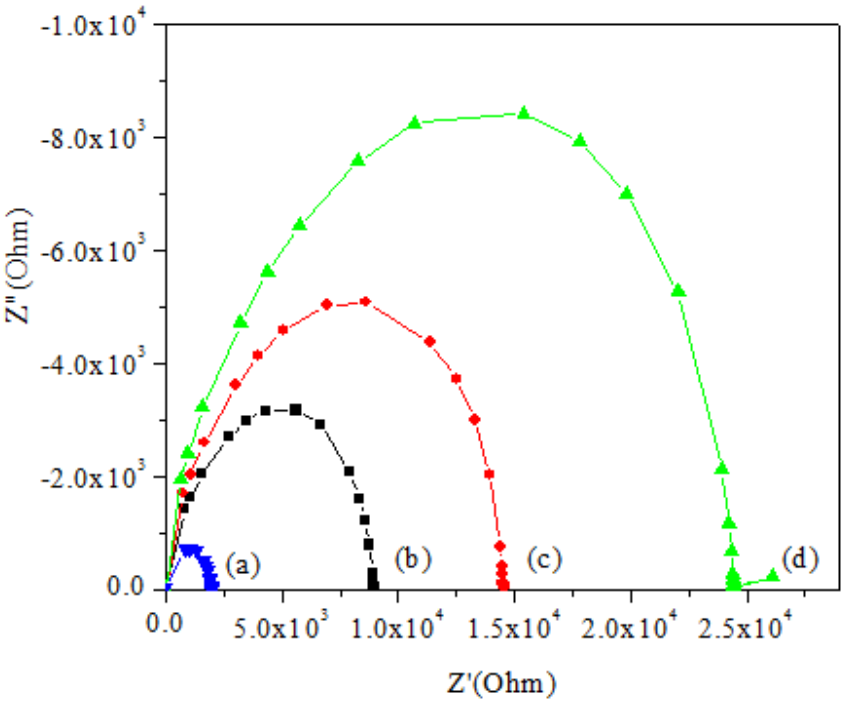

Fig. 3: **Impedance spectrum of (a) $La_{9.33}Si_6O_{26}$, (b) $La_{9.33}Si_{5.7}Sn_{0.3}O_{26}$, (c) $La_{9.33}Si_{5.9}Sn_{0.1}O_{26}$ and (d) $La_{9.33}Si_{5.5}Sn_{0.5}O_{26}$ at 973 K.**

Table 2
Conductivity of $La_{9.33}Si_6O_{26}$, $La_{9.33}Si_{5.9}Sn_{0.1}O_{26}$, $La_{9.33}Si_{5.7}Sn_{0.3}O_{26}$ and $La_{9.33}Si_{5.5}Sn_{0.5}O_{26}$ at 873-973 K.

Temperature (K)	$La_{9.33}$ $Si_{5.9}$ $Sn_{0.1}O_{26}$ (S/cm)	$La_{9.33}$ $Si_{5,7}Sn_{0.3}$ O_{26} (S/cm)	$La_{9.33}Si_{5.5}Sn_{0.5}O_{26}$ (S/cm)	$La_{9.33}Si_6O_{26}$ (S/cm)
973	4.62×10^{-06}	4.75×10^{-05}	2.63×10^{-05}	$2,13 \times 10^{-4}$
923	2.82×10^{-06}	2.93×10^{-05}	1.50×10^{-05}	$1,37 \times 10^{-4}$
873	9.96×10^{-07}	1.64×10^{-05}	8.00×10^{-06}	$8,34 \times 10^{-5}$

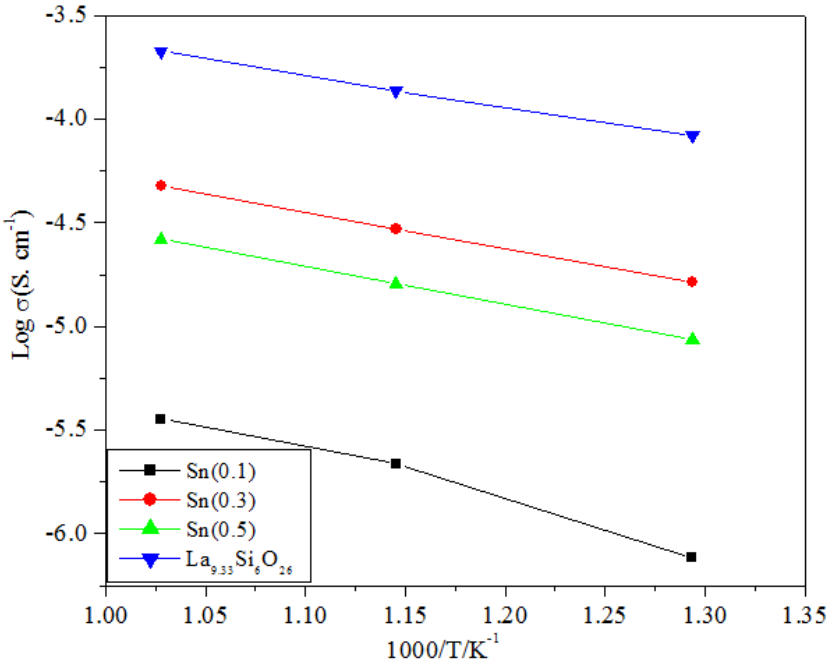

Fig. 4: **Arrhenius plots of total conductivity of $La_{9.33}Si_{6-x}Sn_xO_{26}$ (x = 0.1; 0.3; 0.5) ceramics after sintering at 1773 K.**

Table 3
Activation energy of $La_{9.33}Si_{5.9}Sn_{0.1}O_{26}$, $La_{9.33}Si_{5.7}Sn_{0.3}O_{26}$, $La_{9.33}Si_{5.5}Sn_{0.5}O_{26}$ and $La_{9.33}Si_6O_{26}$

Compound	E_a (eV)
$La_{9.33}$ $Si_{5.9}$ $Sn_{0.1}$ O_{26}	0.36
$La_{9.33}$ $Si_{5.7}$ $Sn_{0.3}$ O_{26}	0.34
$La_{9.33}$ $Si_{5.5}$ $Sn_{0.5}$ O_{26}	0.50
$La_{9.33}Si_6O_{26}$	0.65

Conclusion

Sn(IV) doped Apatite-type $La_{9.33}Si_{6-x}Sn_xO_{26}$ (x: 0.1; 0.3; 0.5) ceramics were prepared via hydrothermal route. All the ceramics consist only of a hexagonal apatite structure with a space group *P63/m*; however, ceramics are composed of second phase La_2SiO_5. The highest total conductivity was obtained from $La_{9.33}Si_{6x}Sn_xO_{26}$ with x = 0.3.

Acknowledgement

We would like to thank the DIKTI (PDUPT No. 718/UN6.3.1/PL/2017) for funding this research.

References

1. Noviyanti A.R., Prijamboedi B., Marsih I.N. and Ismu I., Hydrothermal Preparation of Apatite-Type Phases $La_{9.33}Si_6O_{26}$ and $La_9M_1Si_6O_{26.5}$ (M = Ca, Sr, Ba), *ITB Journal of Science*, **44(2)**, 193-203 **(2012)**

2. Sansom J.E.H., Tolchard J.R., Slater P.R. and Islam M.S., Synthesis and structural characterisation of the apatite-type phases $La_{10-x}Si_6O_{26+z}$ doped with Ga, *Solid State Ionics*, **167(1-2)**, 17-22 **(2004)**

3. Cao X.G., Jiang S.P. and Li Y.Y., Synthesis and characterization of calcium and iron co-doped lanthanum silicate oxyapatites by sol–gel process for solid oxide fuel cells, *Journal of Power Sources*, **293**, 806-814 **(2015)**

4. Cao X.G. and Jiang S.P., Effect of Sr and Al or Fe co-doping on the sinterability and conductivity of lanthanum silicate oxyapatite electrolytes for solid oxide fuel cells, *International Journal of Hydrogen Energy*, **39(33)**, 19093-19101 **(2014)**

5. León-Reina L., Porras-Vázquez J.M., Losilla E.R. and Aranda M.A., Interstitial oxide positions in oxygen-excess oxy-apatites, *Solid State Ionics*, **177(15-16)**, 1307-1315 **(2006)**

6. León-Reina L., Porras-Vázquez J.M., Losilla E.R. and Aranda M.A., Phase transition and mixed oxide-proton conductivity in germanium oxy-apatites, *Journal of Solid State Chemistry*, **180(4)**, 1250-1258 **(2007)**

7. Xiang J., Liu Z.G., Ouyang J.H., Zhou Y. and Yan F.Y., Synthesis and electrical conductivity of $La_{10}Si_{5.5}B_{0.5}O_{27+\delta}$ (B= In, Si, Sn, Nb) ceramics, *Solid State Ionics*, **220**, 7-11 **(2012)**

8. Dai L., Yang G., Zhou H., He Z., Li Y. and Wang L., Mixed potential NH_3 sensor based on Mg-doped lanthanum silicate oxyapatite, *Sensors and Actuators B: Chemical*, **224**, 356-363 **(2016)**

9. Kendrick E., Knight K.S. and Slater P.R., Ambi-site substitution of Mn in lanthanum germanate apatites, *Materials Research Bulletin*, **44(8)**, 1806-1809 **(2009)**

10. Chefi S., Madani A., Boussetta H., Roux C. and Hammou A., Electrical properties of Al-doped oxyapatites at intermediate temperature, *Journal of Power Sources*, **177(2)**, 464-469 **(2008)**

11. Noviyanti A.R., Prijamboedi B., Marsih I.N., Mukti R.R. and Ismunandar, Conductivity and Solid State ^{29}Si NMR studies of apatite-type of lanthanum silicate prepared by hydrothermal method, In ICICI-BME, Bandung Indonesia, IEEE **(2011)**

12. Panteix P.J., Julien I., Abelard P. and Bernache-Assollant D., Influence of porosity on the electrical properties of $La_{9.33}(SiO_4)_6O_2$ oxyapatite, *Ceramics International*, **34(7)**, 1579-1586 **(2008)**

13. Islam M.S., Tolchard J.R. and Slater P.R., An apatite for fast oxide ion conduction, *Chemical Communications*, **13**, 1486-1487 **(2003)**.